Food Hydrocolloids 139 (2023) 108491

Contents lists available at ScienceDirect

Food Hydrocolloids

journal homepage: www.elsevier.com/locate/foodhyd

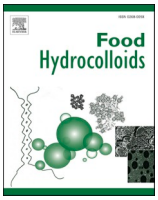

The relationship between starch structure and digestibility by time-course digestion of amylopectin-only and amylose-only barley starches

Wenxin Liang [a,1], Li Ding [a,1], Ke Guo [a], Yang Liu [b], Xiaoxia Wen [b], Jacob Judas Kain Kirkensgaard [c,d], Bekzod Khakimov [d], Kasper Enemark-Rasmussen [e], Kim Henrik Hebelstrup [f,g], Klaus Herburger [h], Xingxun Liu [i], Staffan Persson [a,j], Andreas Blennow [a,*], Yuyue Zhong [a,**]

[a] Department of Plant and Environmental Sciences, Faculty of Science, University of Copenhagen, Denmark
[b] College of Agronomy, Northwest A&F University, Yangling, 712100, Shaanxi, China
[c] Niels Bohr Institute, University of Copenhagen, Universitetsparken 5, 2100 Copenhagen, Denmark
[d] Department of Food Science, University of Copenhagen, DK-1958, Frederiksberg C, Denmark
[e] Department of Chemistry, Technical University of Denmark, DK-2800, Kemitorvet, Building 207 Kgs, Lyngby, Denmark
[f] Department of Agroecology, Aarhus University, Flakkebjerg, Denmark
[g] Plantcarb Aps, Vedbæk, Denmark
[h] Institute of Biological Sciences, University of Rostock, Germany
[i] Lab of Food Soft Matter Structure and Advanced Manufacturing, College of Food Science and Engineering, Nanjing University of Finance and Economics, Nanjing, 210023, China
[j] Joint International Research Laboratory of Metabolic & Developmental Sciences, State Key Laboratory of Hybrid Rice, SJTU-University of Adelaide Joint Centre for Agriculture and Health, School of Life Sciences and Biotechnology, Shanghai Jiao Tong University, Shanghai, China

ARTICLE INFO

Keywords:
In vitro time-course digestion
Digestogram
Amylose-only barley starch
Multi-scale structure

ABSTRACT

The multi-scale structural dynamics of amylopectin-only barley starch (APBS), normal barley starch (NBS), and amylose-only barley starch (AMBS) digested with amylolytic enzymes for 120 min were investigated in this study. For all starches, 0–20 min was identified as a rapid digestion stage, followed by a 20–120 min slow digestion. For APBS and NBS, the content of short chains (DP $\leq$ 12) and the thickness of crystalline and amorphous nano-lamellae increased, whereas the crystallinity decreased, and pores were generated on the granular surface during the rapid digestion stage. At the following slow digestion stage, the branching degree and relative amount of double helices increased, the crystalline and lamellar structures were lost, and the hydrolyzed starch segments aggregated. For AMBS, the rapid digestion stage was characterized by an increased content of short chains (DP $\leq$ 8) and B-type crystals and decreased amounts of V-type crystals. Furthermore, the lamellar and granular structures were lost, and digestion residues aggregated during the first stage of AMBS, which were formed in the second digestion stage of APBS and NBS. The second slow digestion stage of AMBS was characterized by an increased branching degree and a decreased relative content of single helices. It is suggested that the aggregated digestion residues at the initial digestion stage are the main reason for the overall low digestibility of AMBS.

1. Introduction

Barley (*Hordeum vulgare* L.) is among the most important cereal crop in the world, particularly in Asia and Northern Africa. Due to its high dietary fiber content and health benefits such as lowering the glycemic index and blood cholesterol (Zeng et al., 2018), barley-based foods are becoming increasingly popular as a substitute partially or wholly for currently used cereal grains such as wheat (*Triticum aestivum*), oat (*Avena sativa*), rice (*Oryza sativa*), and maize (*Zea mays*) (Baik & Ullrich, 2008). Starch is the main component of the barley grain, and plays an

* Corresponding author.
** Corresponding author.
E-mail addresses: abl@plen.ku.dk (A. Blennow), yuyuezhong93@163.com (Y. Zhong).
[1] The authors contributed the same.

https://doi.org/10.1016/j.foodhyd.2023.108491
Received 12 October 2022; Received in revised form 3 January 2023; Accepted 16 January 2023
Available online 23 January 2023

important role for the taste, texture, and nutrition of barley foods. Understanding barley starch digestion is critical for producing low-glycemic index barley foods.

Starch granules can be described at different structural, and hierarchical levels, including molecular linkages forming amylose (AM) and amylopectin (AP) macromolecules, that form nano-lamellar structures, semi-crystalline structures, eventually leading to the formation of concentric shells of growth rings, blocklets, and finally the granular structure (Bertoft, 2017; P. Chen, Xie, Zhao, Qiao, & Liu, 2017). The packing of the chain segments in the starch granule can be described according to the so-called backbone model (Bertoft, 2017), where AP is proposed to include long flexible chains, so-called B2-and B3-chains, from which short-branched building blocks of A-, and B-chains extend. The short AP chains extend from branched "building blocks" to form double helices, while long AP chains mainly make up the backbone. Starches from different botanical sources typically display structural differences and therefore different digestibility. For example, potato starch, with a B-type crystalline structure, has higher enzymatic resistance than cereal starches (Butterworth, Warren, & Ellis, 2011).

A better understanding of how the organization of starch at different levels affects its enzymatic digestibility, glycemic index, and calorie input are crucial because obesity is becoming an epidemic in the 21st century, which can be linked to different health impairments, like type-2 diabetes and cardiovascular diseases (Guo, Tan, & Kong, 2021). Hence, developing new types of starch that facilitate a lower/slower intake of calories and sugar can be a powerful tool for preventing lifestyle diseases. In this context, resistant starch (RS) is becoming an interesting type of starch because it resists digestion in the small intestine, helps controling the glycemic level, and reduces inflammation (Noor, Gani, Jhan, Jenno, & Arif Dar, 2021). The RS content is related to different structural parameters of starch (Bertoft, 2017; Yao et al., 2019), and the AM content (AC) is one of the most critical factors (Li, Gidley, & Dhital, 2019).

Several studies have investigated the RS contents from different types of raw and modified starches, and different strategies have been used to test and elevate the RS contents (Jiang, Campbell, Blanco, & Jane, 2010; Li, Jiang, Campbell, Blanco, & Jane, 2008; Ma et al., 2018; Witt, Gidley, & Gilbert, 2010; Zhang, Sofyan, & Hamaker, 2008; Zhong, Qu et al., 2022; Zhong, Tai, et al., 2022). However, the information on the digestive process of starches and how it is affected by the starch structure are still scarce, which is a fundamental problem for fully exploiting starches' nutritional potential because it limits our ability to develop crops with high-RS starch contents. For example, significant changes in the molecular chain size distribution (e.g., AM chain length), crystalline structures, and nano-lamellar structures are decisive for the digestion process of maize starches with different AC (Shrestha et al., 2012; Witt et al., 2010). A so far neglected phenomenon is the potential dynamic changes in starch structure taking place during amylolytic digestion. Questions that need to be addressed include how the AP and AM, including their degradation products, specifically change during digestion and affect the higher levels of starch structure. To investigate this, we took advantage of the remarkable variations in the digestion profiles of granular-state amylopectin-only barley starch (APBS) and amylose-only barley starch (AMBS) (Zhong, Tian, et al., 2021), providing us with suitable substrates for studying whether and how AM and AP determine the starch digestibility. It is hypothesized that AM and AP molecules exert different roles in determining the digestion process of granular starch.

Hence, to verify this hypothesis, three types of barley starches with AC 0% (APBS), 30% (amylose-only barley starch; NBS), and 99% (AMBS) were selected, and the multi-scale structures of these starches before, during, and after an *in vitro* simulation digestion process were analyzed.

2. Materials and methods

2.1. Materials

Three types of barley starches were used: amylopectin-only barley starch (APBS, cv. Cinnamon, kindly provided by Lantmännen SW Seed, Sweden), normal barley starch (NBS, cv. Golden Promise), and Amylose-only barley starch (AMBS, a starch branching enzyme RNAi line in the Golden Promise background (Carciofi et al., 2012). Their AC was determined by the iodine complexation protocol as described before (Carciofi et al., 2012), in which the AC of WBS, NBS, and AOBS was measured as 1.2%, 29.0%, and 99.8%, respectively. Isoamylase (E-ISAMY, 280 U mL^{-1}) and pullulanase (E-PULKP, 650 U mL^{-1}) were from Megazyme (Ireland). Pancreatin (Cat. No. P7545) and amyloglucosidase (Cat. No. A7095) were from Sigma (St. Louis, MO, USA).

2.2. In vitro digestion and sample collection

The digestion of raw starch samples was analyzed as reported before (Zhang et al., 2008; Zhong, Liu, Qu, Blennow, et al., 2020). In brief, starch samples (100 mg) were mixed with 5 mL water and 10 mL sodium acetate buffer (0.1 M, pH 5.2) by gentle stirring, and equilibrated at 37 °C for 30 min. The digestion process was started by adding 2.5 mL reaction buffer (2.5 mL 0.1 M sodium acetate buffer, 18.75 mg pancreatin, and 13.4 μL amyloglucosidase). Aliquots (0.1 mL) were withdrawn at 0, 10, 20, 40, 60, 80, 100, and 120 min, and the reaction was terminated by adding 1 mL of 95% (v/v) aqueous ethanol. The released glucose was quantified with the Megazyme GOPOD kit. The digestion profiles of three types of barley starches (Fig. 1) suggested that all starches had two digestion stages: rapid digestion stage in 0–20 min and slow digestion stage in 20–120 min. Hence, starch residues after 10, 20, 60, and 120 min were collected after inactivating enzymes with 95% ethanol, covering the two digestion stages; samples were freeze-dried after washing three times with 40 ml of MilliQ water. A "pseudo first-order kinetics" plot was generated to calculate the digestion rate constant (k) and digested starch content (C∞) as described before (Cheng, Hu et al., 2021). Fitting data are shown in Fig. S1.

2.3. Size-exclusion chromatography (SEC)

The molecular size distributions of raw and digested starch samples were analyzed by size-exclusion chromatography (SEC-TDA, Viscotek,

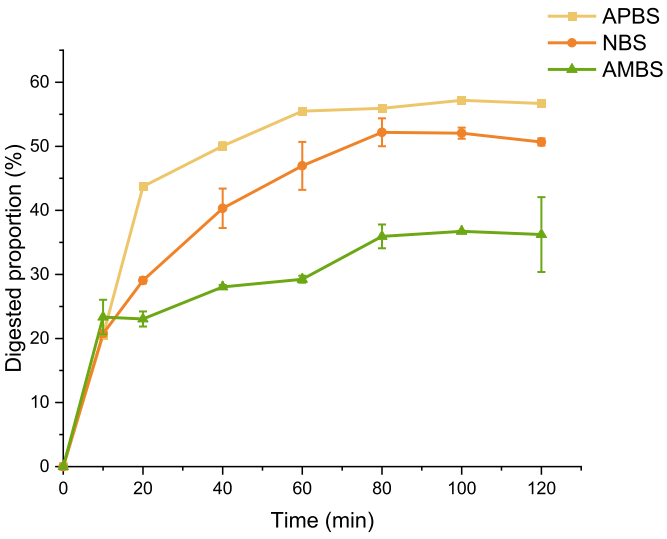

Fig. 1. *In vitro* digestion profiles of barley starches with different amylose content. APBS: Amylopection-only barley starch; NBS: Normal barley starch; AMBS: Amylose-only barley starch.

Malvern, UK) instrument equipped with tandem GS-520HQ/GS-320HQ Shodex columns attached to a TDA302 detector array. The eluent was ammonium formate (10 mM), set at a flow rate of 0.5 mL/min and column temperature of 60 °C (Zhong, Keeratiburana, et al., 2021). Starch (5 mg) and 20 μL 2M sodium hydroxide (NaOH) were mixed and stored at 4 °C overnight, followed by a dilution to 1 mg mL^{-1} before incubating at 80 °C for 5 h. The solubilized starches were centrifuged at 20,000 *g* for 5 min before injecting 50 μL supernatant onto the SEC-TDA system.

2.4. High-performance anion exchange chromatography-pulsed amperometric detection (HPAEC-PAD)

Starch samples (5 mg mL^{-1}) were gelatinized at 99 °C (NBS, APBS) or 130 °C (AMBS) for 0.5 h and debranched with 2 μL isoamylase and 2 μL pullulanase at 40 °C for 3 h. 10 μL of the sample was injected onto a CarboPac PA-200 column attached to an HPAEC-PAD (Dionex, Sunnyvale, CA, USA) system. The digestion products were quantified following the detector response correction (Song et al., 2020; Wu, Morell, & Gilbert, 2013).

2.5. Wide-angle X-ray scattering (WAXS) and small-angle X-ray scattering (SAXS)

The samples were stored at 90% relative humidity overnight and analyzed by a SAXSLab instrument (JJ-X-ray, Copenhagen, Denmark) equipped with a 100 XL + microfocus sealed X-ray tube (Cu-K_α radiation, Rigaku, The Woodlands Texas, USA) and a 2D 300 K Pilatus detector (Dectris Ltd, Baden, Switzerland). All conditions were set as reported before, and the relative crystallinity was calculated (Zhong, Keeratiburana, et al., 2021).

SAXS analysis was performed with the same instrument as above, following the method as described before (Kuang et al., 2017). The wavelength of the incident X-ray for SAXS was 1.03 Å, and the sample-to-detector distance was 2.6 m. The scattering vector of SAXS was calibrated using a beef tendon specimen as standard material. The air and water scattering were subtracted from the original SAXS data. The normalized 1D correlation function γ1(r) was used to obtain the thickness of crystalline (dc) and amorphous (da) lamella.

2.6. ^{13}C Nuclear magnetic resonance (^{13}C NMR)

Solid-state ^{13}C Cross Polarization/Magic Angle Spinning Nuclear Magnetic Resonance Spectroscopy (CP/MAS NMR) was performed at a ^{13}C frequency of 75.4 MHz using a Bruker AV-300 spectrometer, with the parameter settings as described before (Zhong, Li et al., 2021). Amorphous AMBS powder was prepared by gelatinizing starch suspensions (1% w/v) at 140 °C for 60 min before lyophilization. The relative contents of the single helix (102–103 ppm), double helix (99–101 ppm), and amorphous region were calculated by decomposing the spectrum of native starch into its respective amorphous and ordered subspectra by subtraction at 84 ppm (Tan, Flanagan, Halley, Whittaker, & Gidley, 2007).

2.7. ^{1}H Nuclear magnetic resonance (^{1}H NMR)

Starch (5 mg mL^{-1}) was heated in deuterium oxide at 99 °C for 1 h, lyophilized, and re-dissolved in a mixture solution of 1 mL 10% deuterium oxide and 90% DMSO at 99 °C for 1 h. One-dimensional ^{1}H NMR spectra acquired on 500 MHz NMR spectrometers (Bruker Avance III) from Bruker (Bruker Biospin, Rheinstetten, Germany) were used to analyze the signals representing anomeric protons of α-1,4 linkage α-1,6 linkage, α-anomeric reducing end protons, and β-anomeric reducing end protons of samples (Gidley, 1985; Zhong, Keeratiburana, et al., 2021). Areas of signals representing anomeric protons were quantified by SigMa software (Khakimov, Mobaraki, Trimigno, Aru, & Engelsen, 2020).

2.8. Scanning electron microscopy (SEM)

Starch samples were sprinkled on double-sided adhesive tape mounted on an aluminum plate, then coated with a thin gold film and observed using an FEI Quanta 200 field emission scanning electron microscope (FE-SEM).

2.9. Statistical analysis

SPSS V. 19.0 software (SPSS Inc., Chicago, IL) and the analysis of variance (ANOVA) with Duncan at the 95.0% confidence level were used to analyze the mean and standard deviation of data. *In vitro* digestion, SEC, HPAEC-PAD, WAXS, and DSC were all performed in triplicate, and ^{13}C NMR and ^{1}H NMR were conducted once.

3. Results and discussion

3.1. Digestibility

The digestion profiles of the three types of barley starch (Fig. 1) showed a rapid digestion process during the first 10 min, after which the rate of digestion decreased within the next 100 min. The amount of starch digested within 120 min correlated with the AC: AMBS was less digested during the whole digestion process as compared to APBS and NBS, which is in agreement with previous reports (Zhong, Liu, Qu, Blennow, et al., 2020; Zhong, Qu et al., 2022; Zhong, Tai, et al., 2022). However, the amounts of digested starch for AMBS in the first 10 min were similar to the other two types of starches, demonstrating high amylolytic susceptibility of AMBS during the very initial digestion stage. On the other hand, it has been reported that the starch damage degree is positively correlated with enzyme susceptibility (Li et al., 2018), and thus the original starch damage deree might be another factor affecting the rapid digestion time. After that, the digestion rate of AMBS decreased notably, suggesting an enhanced enzymatic resistance during the digestion process, which might be due to an increased production of slowly digested remnant starch segments (Witt et al., 2010). According to the two stages of digestion i.e., rapid (the first 10 minutes) and slow (the next 100 minutes), found for the three types of starches, two digestion points in each stage were selected to perform a multi scale structural characterization analysis of digested starches. Kinetics analysis in Table 1 is consistent with the description above, showing that increasing AC decreased the digestion rate constant (*k*) and the digested starch content (C∞).

3.2. Molecular structure

Molecular size distribution profiles of the digested starches (Fig. 2) showed a continuously decreasing trend in molecular size for all starches. The elution volume, being roughly negatively correlated with

Table 1
The digestion properties of barley starches with different amylose content.

Sample	Uncooked starch			*k* (min^{-1})	C∞
	RDS (%)	SDS (%)	RS (%)		
APBS	70.0 ± 0.5^{a}	26.5 ± 0.2^{c}	1.5 ± 0.1^{c}	0.035	98.3 ± 0.1^{a}
NBS	24.0 ± 0.8^{b}	44.2 ± 0.1^{a}	14.9 ± 0.6^{b}	0.016	85.7 ± 0.6^{b}
AMBS	23.1 ± 0.5^{b}	29.5 ± 0.6^{b}	47.4 ± 0.1^{a}	0.004	52.6 ± 0.2^{c}

Values are means ± SD. Values with different letters in the same column are significantly different at $p < 0.05$.
APBS: Amylopection-only barley starch; NBS: Normal barley starch; AMBS: Amylose-only barley starch.
k: digestion rate; *C*∞: digested starch content; RDS: rapidly digested starch content; SDS: slowly digested starch content; RS: resistant starch content.

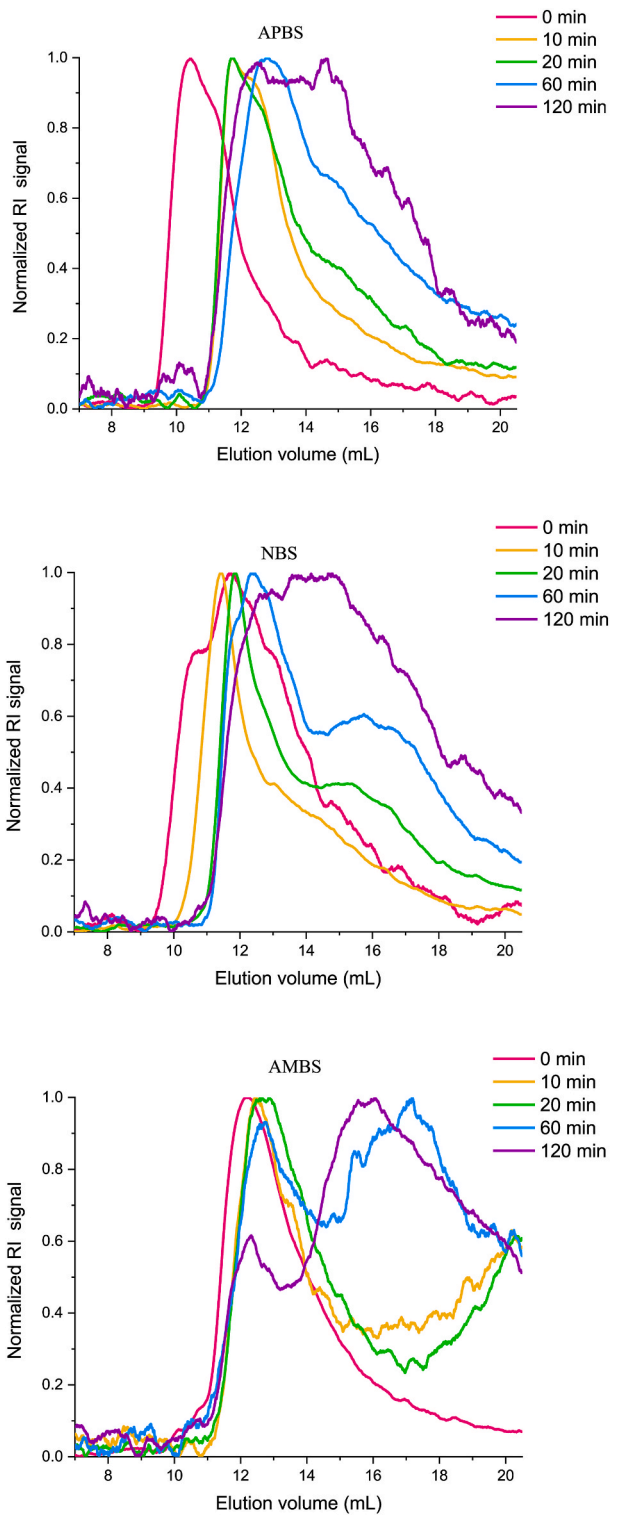

Fig. 2. Molecular weight distributions of raw digested barley starches with different amylose content as analyzed by SEC. Abbreviations as in Fig. 1. The refractive index detector (RI).

the molecular size of the starch macromolecules (Zhong, Herburger, et al., 2021; Zhong, Herburger, et al., 2022), allowed us to discern the wide molecular size distributions for all the barley starches during digestion into two temporal stages: a minor and a major shift of the peak within 0–20 min and 20–120 min digestion, respectively, corresponding to the content of digested starch at the two stages, respectively (Fig. 1). At the first digestion stage, the molecular size of APBS decreased faster than found four NBS and AMBS, while at the next stage, the molecular size of AMBS decreased faster than that of NBS and APBS.

Chain lengths distribution (CLD) profiles of the AP fraction (Fig. 3) showed an increase in short chains and a decrease in long chains during digestion. Hence, at the rapid digestion stage (0–20 min) of APBS, the content of AP chains with DP 13-60 decreased, and the content of AP chains with DP $\leq$ 12 increased, with a shift in the peak maximum from DP 6 at 10 min to DP 3 at 20 min digestion. In the following slow digestion process, the relative content of AP short side chains with DP $\leq$ 12, especially the chains with DP 1–3, decreased, indicating further amyloglucosidase-catalyzed hydrolysis of α-1,6 bonded glucose,

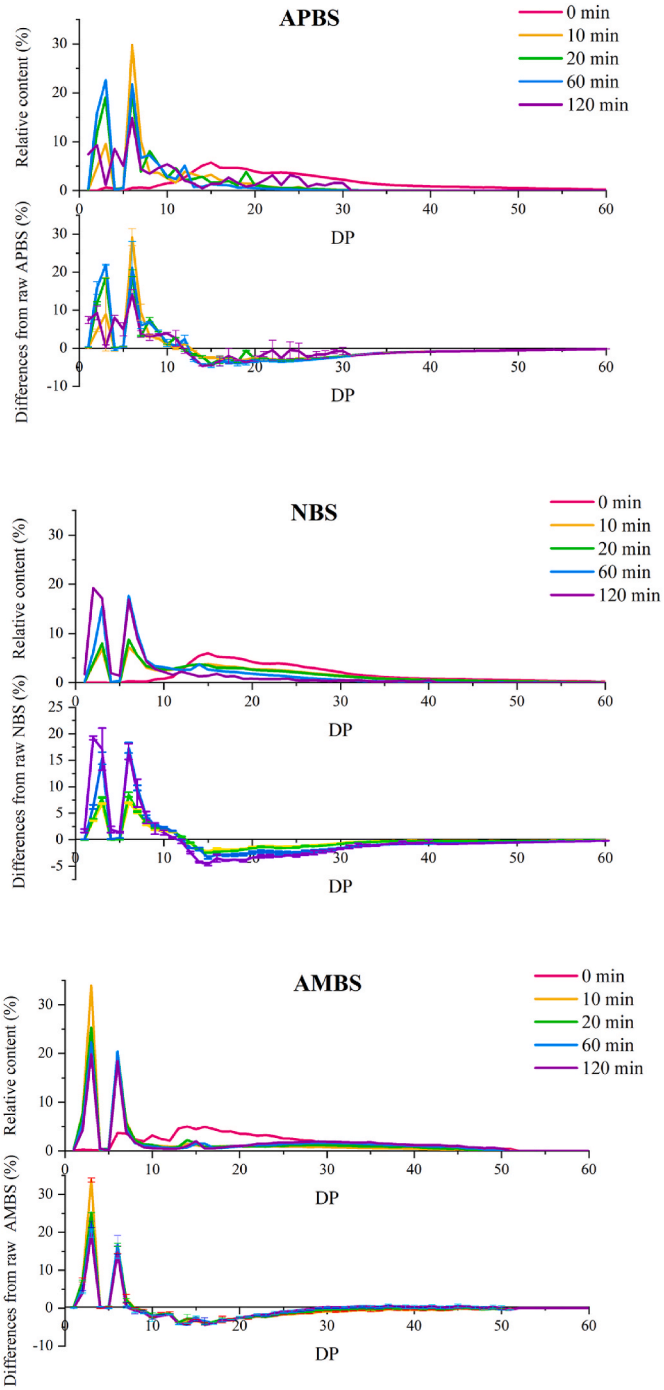

Fig. 3. Chain lengths distributions of debranched digested barley starches with different amylose content as analyzed by HPAEC-PAD. Abbreviations as in Fig. 1. Degree of polymerization (DP).

maltose, and maltotriose stubs of AP side chains. In the whole digestion process of NBS, there was a continuous tendency for long AP chains with DP 13-60 to decrease, while short AP chains with DP 1–12 increased, especially two peaks at DP 3 and DP 6, in which the second digestion stage (20–120 min) showed a higher hydrolysis level of long AP chains as compared to the first stage (0–20 min). Hence, AP chains with DP 13–60 in APBS and NBS were the main substrates of pancreatin and amyloglucosidase during digestion. However, in the digestion process of AMBS, the content of branched chains with DP 8-51 decreased, and the content of branched chains with DP 1–7 increased, suggesting that these two enzymes mainly hydrolyzed branched chains in the DP 8–51 range. A suitable length of starch chains is important for their binding to the active side of the amylolytic enzyme (Chi et al., 2021; Gilles, Astier, Marchis-Mouren, Cambillau, & Payan, 1996; Zhong, Herburger, et al., 2021; Zhong, Keeratiburana, et al., 2021). Thus, the generation of short AP chains (DP $\leq$ 12) in all barley starches during digestion might have retarded the enzymatic digestion, possibly because of their branched nature.

3.3. Degree of branching and helical structure

For the degree of branching (DB), ^{1}H NMR data (Fig. 4, Table 2) showed a negative correlation between the AC and DB of the raw starches, which is consistent with that starch with very high AC is mainly linear (Li et al., 2019). The increase in DB was also negatively correlated with AC: APBS showed an increase in DB at both digestion stages; however, NBS only exhibited a significant increase in DB within the slow digestion period, and there was only a slight enhancement of DB in the later digestion process of AMBS. Both pancreatic α-amylase and amyloglucosidase are amylases that are mainly hydrolyzing α-(1,4) bonds of AM and AP molecules, although amyloglucosidase is capable also of hydrolyzing α-(1,6) bonds, albeit at a much slower rate (Ao et al., 2007; Zhong, Xu et al., 2022). Hence, the increase in DB of APBS during the whole digestion process suggests that the enzymes were mainly active on the α-(1,4) linkages (Fig. 4) and thus increased the relative amount of α-(1,6) linkages. However, the minor changes in DB of the AM-containing starches, NBS, and AMBS, at the rapid digestion stage indicated that the rates of hydrolysis of α-(1,4) linkages and α-(1,6) linkages were similar at this stage. At the slow digestion stage, both NBS and AMBS showed significant increases in DB, implying that the hydrolysis rate of α-(1,4) acting enzymes was higher than that of the α-(1,6) linkages. For AMBS, it is suggested that this is associated with a higher content of 'AM-like' material inside the granules, which substitutes AP molecules functioning as the granular backbone structure. 'AM-like' material is a new type of AM with somewhat higher DB than normal AM. This material is suggested to be generated from AP when isoforms of the starch branching enzymes are downregulated (Zhong, Liu, Qu, Li, et al., 2020; Zhong, Qu et al., 2022).

The relative helical and amorphous contents of the solid samples as measured by solid-state ^{13}C Cross Polarization/Magic Angle Spinning Nuclear Magnetic Resonance Spectroscopy (CP/MAS NMR)(Table 2) suggested that an increased AC induced a lower relative content of double helices and a higher relative content of single helices and amorphous material in the raw barley starch granules. Digestion decreased the relative amounts of amorphous materials of APBS, suggesting that the amorphous region was predominately attacked during digestion, especially at the later slow digestion stage. The relative content of double helices increased during digestion, which can be explained by two possible mechanisms. (I) The amorphous regions were severely attacked, and thus the relative content of the double helices increased. (II) New double helical structures were formed due to the cleavage of AP backbone chains supported by AP CLDs (Fig. 3) and the helical entanglement of these cleaved chains. During the first digestion stage, it was found a minor decrease in the relative content of double helices and an increase in the relative content of single helices in NBS, mainly showing that helical and non-helical regions occur side-by-side

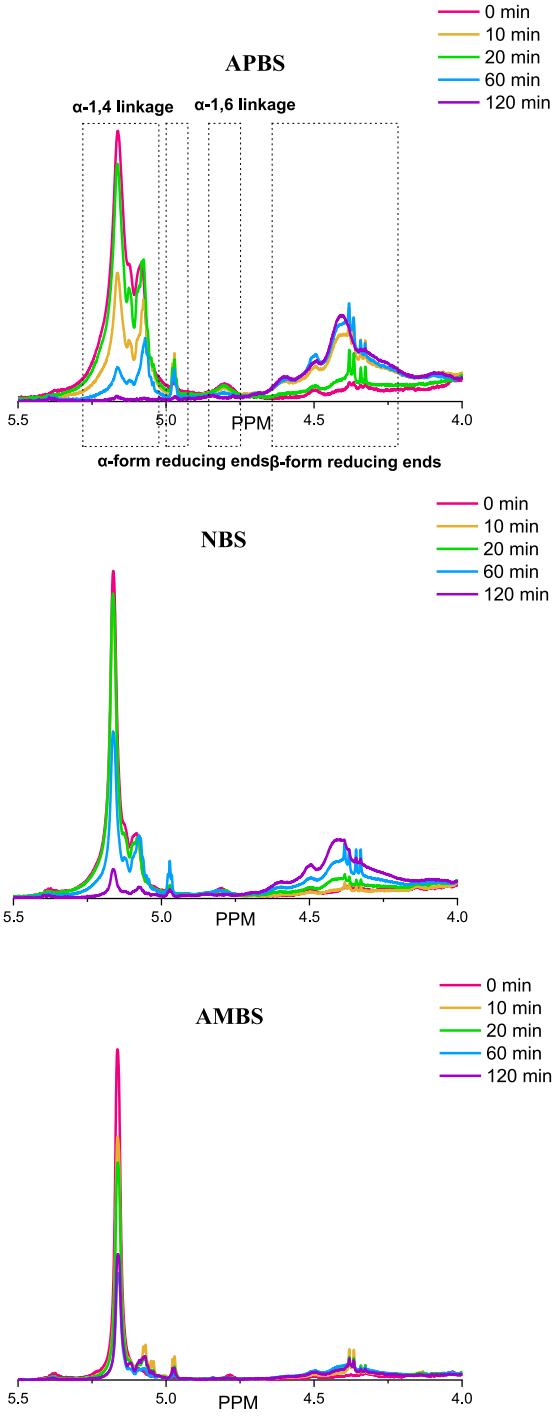

Fig. 4. Branching degree of digested barley starches with different amylose content as analyzed by ^{1}H NMR. Abbreviations as in Fig. 1. Parts per million (PPM).

during the process, in agreement with a previous study on normal maize starch (Shrestha et al., 2012). The data for the APBS showed that the double helices are resistant to digestion, and the decreased double helix content in NBS is suggested to be related to the hydrolysis of those helical defects that are related to AM molecules. It has been shown that AM molecules can form double helical structures with AM side chains (Klucinec & Thompson, 1999). Our data suggest that such AM-AP double helical structures are less resistant than AP-AP double helical

Table 2
The aggregation structural parameters of digested barley starches with different amylose content as analyzed by ^{1}H NMR, and ^{13}C NMR.

Sample	Digestion time (min)	Branching degree (%)	The content of double helix (%)	The content of single helix (%)	The content of amorphous materials (%)
APBS	0	7.8	48	0	52
	10	10.6	49	3	48
	20	8.0	50	4	46
	60	20.6	64	0	36
	120	35.3	68	0	32
NBS	0	3.3	38	8	54
	10	3.2	34	12	54
	20	3.0	35	14	51
	60	4.9	33	16	51
	120	10.8	38	0	62
AMBS	0	1.6	16	22	62
	10	1.5	17	12	71
	20	1.5	16	10	74
	60	2.5	17	4	72
	120	2.2	18	3	79

APBS: Amylopection-only barley starch; NBS: Normal barley starch; AMBS: Amylose-only barley starch.
The analysis of these parameters was performed once after testing raw starches with good replication (Fig. S1).

structures. However, an increase in the relative content of the amorphous region of NBS was found in the 120 min digestion samples, implying a higher level of disruption in the crystalline region. This was associated with the loss of single helical structures, which might have been caused by the AM single helical matrix being less resistant than the AP double helical matrix. The significantly decreased content of AP long chains (Fig. 3) in the whole digestion process of NBS suggests that new double helices were formed during the digestion. Hence, the remaining relative content of double helices in NBS during digestion indicated a dynamic balance of double helix hydrolysis and formation. The increased amounts of single helices during digestion suggest that shorter AM chains mostly formed single helical structures. The raw AMBS granules contained both double helix and single helix structures (Table 2), which contrasts with AM's preferred single helix conformation in high-AM starches (Li et al., 2019; Zhong, Tai, et al., 2022). AMBS can be regarded to be composed of two types of AM molecules, mainly linear AM produced by the original granule-bound starch synthase (GBSS) catalyzed AM biosynthesis pathway and more branched 'AM-like' material generated from AP in the aberrant pathway when starch branching is knocked-down by genetic means (Zhong, Qu, et al., 2022). Hence, it is suggested that single helical structures are generated from the first type of AM, and double helices are related to packing side chains of 'AM-like' materials in AMBS. The single helical structure of AMBS was disrupted dramatically once the digestion was initiated, suggesting an amylolytic susceptibility of AM single helices, which was also observed for NBS. Correspondingly, the relative amounts of amorphous materials increased during digestion. The relative content of double helices in AMBS was unchanged throughout the digestion, which might be attributed to the dynamic balance of hydrolysis and formation of AM double helices. During digestion, a minor change in the helical structure has also been found in two types of high-AM maize starches, Gelose 50 and Gelose 80 (Shrestha et al., 2012).

3.4. Lamellar and crystalline structure

The nano-lamellar structure, as deduced from SAXS profiles (Fig. 5), showed disordering of the lamellar structure of all three barley starches during digestion. At the rapid digestion stage, APBS and NBS still displayed a typical 9-nm lamellar repeated structure with a sharp and strong peak at the q value of approximately 0.06 (Å^{-1}) (Fig. 5). Thicker

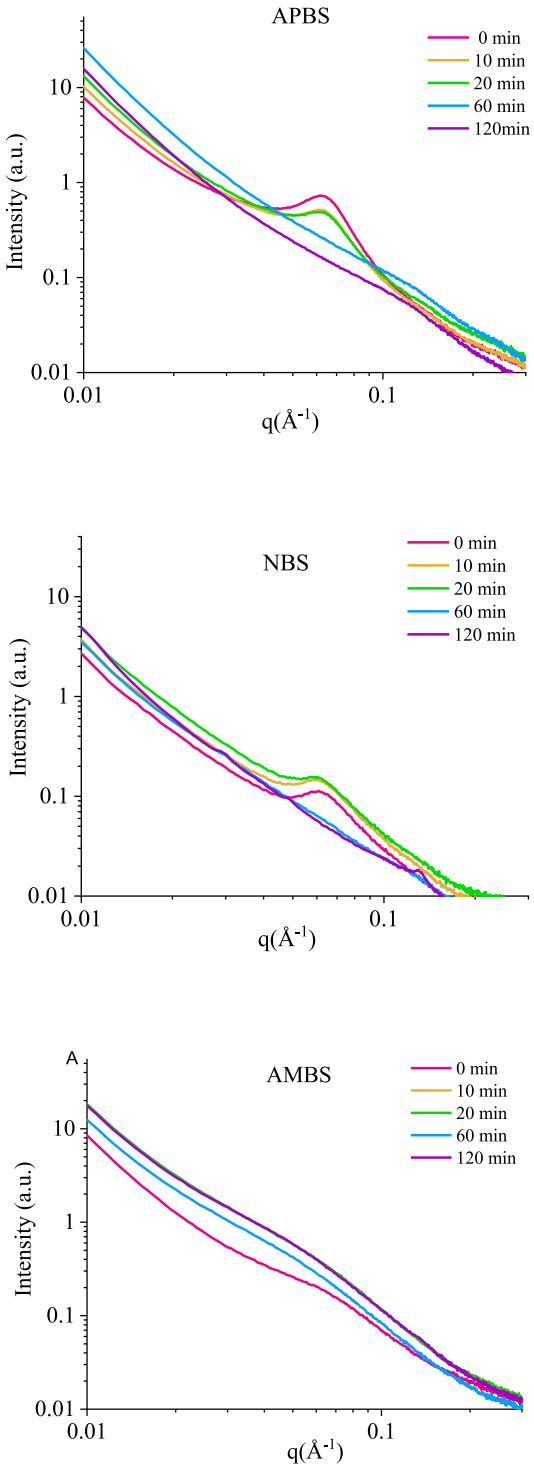

Fig. 5. The lamellar structure profiles of digested barley starches with different amylose content as analyzed by SAXS. Abbreviations as in Fig. 1.

crystalline lamellae (Table S1) suggested a looser lamellar structure due to the hydrolysis of AP connector and backbone chains (Fig. 3). In the slow digestion stage of APBS and NBS, no lamellar peak was found, indicating that the enzymes completely destroyed the ordered lamellar structures of the starch. As expected, raw AMBS displayed a very weak and broad lamellar peak at q value of approximately 0.06–0.07 (Å^{-1}) (Fig. 5) due to AM not being capable of forming well-ordered lamellar

structures (Zhong, Tai, et al., 2022). The weak lamellar structure of AMBS was removed completely once the digestion was initiated (Table S1), corresponding to the disruption of single helical structures (Table 2). This suggests that an increase in AC to very high levels disrupts the stability of lamellar structures by causing crystal defects (Zhong, Liu, Qu, Blennow, et al., 2020), thereby increasing susceptibility for amylolytic cleavage and the lamellar structure.

WAXS profiles (Fig. 6) exhibited a typical A-type crystalline allomorph of APBS and NBS and a mixture of B-type and V-type crystalline allomorphs of AMBS, which is consistent with previous reports (Carciofi et al., 2012; Zhong, Tian, et al., 2021). In the rapid digestion stage, the crystallinity of APBS decreased, implying that the crystalline granular region was already attacked by the enzymes. At the slow digestion stage, no crystallinity of APBS was detected, demonstrating severe disruption of the crystalline parts, although the amorphous parts were also notably attacked by the hydrolytic enzymes (Table 1). However, the remaining high relative content of double helices at this stage suggests that the major substrates of the amylases were not double helices. Hence, it is concluded that the amylases primarily hydrolyzed the AP backbone chains and the connector chains between the backbone chains and double helices, which is consistent with the significant increase in the degree of branching during the digestion period (Table 2). This process leads to the disorder of the double-helical alignment. Therefore, as discussed in section 3.3, it is suggested that there was a slight disruption of both the amorphous and the crystalline regions at the first digestion stage and a severe disruption of both regions at the second stage, i.e., the digestion of APBS entailed a side-by-side hydrolysis pattern in both the amorphous and crystalline regions.

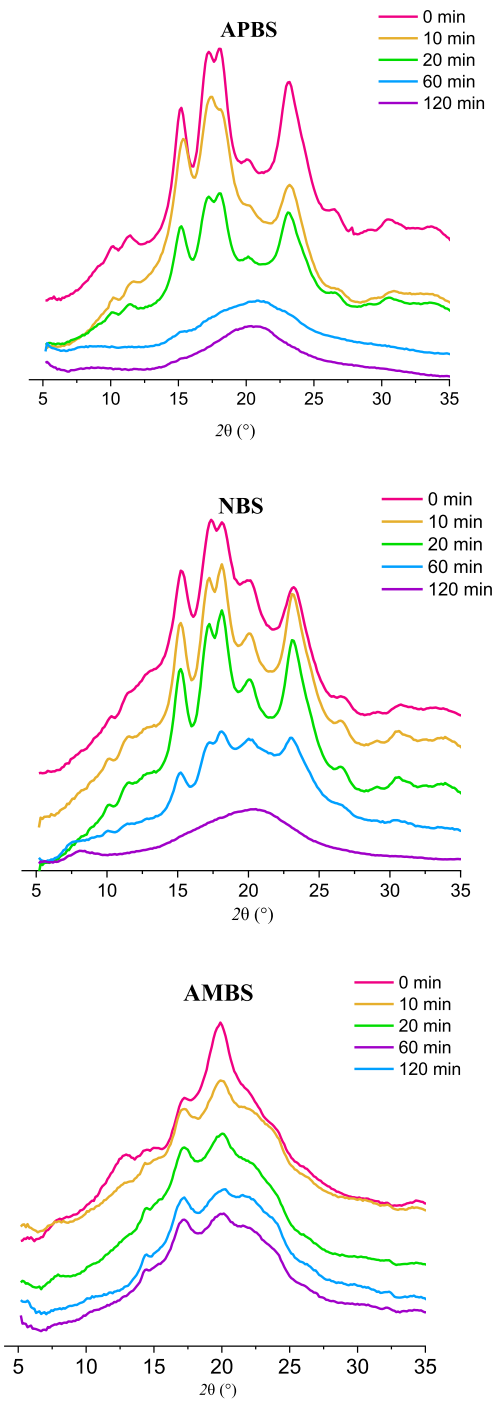

Fig. 6. The crystalline structure profiles of digested barley starches with different amylose content as analyzed by WAXS. Abbreviations as in Fig. 1.

Similarly, for NBS, such a simultaneous hydrolysis pattern resulted in an almost unchanged crystallinity at the rapid digestion stage. However, the crystallinity started to decrease and then became undetectable at the slow digestion stage, conceivably due to the cleavage of AP backbone and connector chains (^{1}H NMR data in Table 2) and the loss of AM single helices (^{13}C NMR data in Table 2). The V-type crystallinity decreased at the first fast digestion stage of AMBS (Table 3), in agreement with the decrease in the single helix relative content of AM (Table 2). The B-type crystallinity increased at this stage, which is possibly attributed to the attack of the amorphous region (Table 3) and the increase in the relative amounts of B-type crystals composed of the side chains in the AM-like molecules. The data indicate there might be a conversion from the V-type crystalline polymorph to the B-type crystalline polymorph, suggesting extensive molecular reorganization of some content. However, it has been reported that the V-type crystalline polymorph is the main reorganized structure of AM molecules in gelatinized starch systems (Zhong, Tai, et al., 2022), which is inconsistent with the decreased content of V-type crystal in NBS and AMBS during digestion (Table 3). A possible explanation is that the V-type crystal in granular starch is less enzymatically resistant than the B-type crystal, and thus the generated new V-type crystals were hydrolyzed and thus were not detected by ^{13}C NMR.

3.5. Morphology

As deduced by SEM (Fig. 7), samples depict more irregular and aggregated granular shapes for AMBS than for APBS and NBS. During the initial 20 min digestion of ABPS, large channels and grooves were formed in the intact granules, after which the starch granules were thoroughly disrupted and the granular segments re-aggregated at the 20–120 min stage, which was associated with a decrease and loss of crystallinity (Fig. 6 and Table 2). A similar tendency was found for the digestion process of NBS; however, only a few porous starch granules were found after 120 min digestion of the NBS samples, most likely due to its higher enzymatic resistance. The irregular APBS granules were rapidly disrupted and reorganized into large aggregates at the initial digestion stage, corresponding to the loss of lamellar structure in that period (Table S1), supporting the reorganization of the AM molecules. However, according to the digestion profile (Fig. 1), such aggregates were enzymatically highly resistant. It has been reported that the slow digestion of high-AM starches can be attributed to the absence of extensive pores and channels on the granular surface, thereby preventing the binding of enzymes during the digestion (Shrestha et al., 2012). However, our study showed that the low amylolytic susceptibility of AMBS was also attributed to AM reorganization. Such reorganization can be induced by the release of structural tension by the amylolytic activity in the AMBS granules, composed of conglomerated small granules in “sheaths” (Shaik et al., 2016).

Table 3
The crystalline structural parameters of digested barley starches with different amylose content as analyzed by WAXS.

Sample	Digestion time (min)	A-type crystallinity (%)	B-type crystallinity (%)	V-type crystallinity (%)	Total crystallinity (%)
APBS	0	31.6 ± 2.0[a]	0.0	1.3 ± 0.3[a]	32.9 ± 1.7[a]
	10	24.4 ± 0.2[b]	0.0	1.5 ± 0.3[a]	25.9 ± 1.0[b]
	20	23.5 ± 0.5[c]	0.0	1.2 ± 0.1[a]	24.7 ± 0.5[b]
	60	N. D	N. D	N. D	N. D
	120	N. D	N. D	N. D	N. D
NBS	0	18.5 ± 1.0[b]	0.0	1.8 ± 0.1[b]	20.3 ± 1.0[c]
	10	21.6 ± 1.0[a]	0.0	2.1 ± 0.0[a]	23.7 ± 0.9[a]
	20	19.7 ± 0.4[b]	0.0	1.6 ± 0.1[b]	21.3 ± 0.3[b]
	60	11.4 ± 0.1[c]	0.0	1.6 ± 0.3[b]	13.0 ± 0.3[d]
	120	N. D	N. D	N. D	N. D
AMBS	0	0.0	5.3 ± 0.0[c]	9.4 ± 1.0[a]	14.7 ± 1.0[a]
	10	0.0	8.2 ± 0.5[b]	5.2 ± 0.9[b]	13.4 ± 0.4[a]
	20	0.0	8.5 ± 0.1[b]	2.2 ± 0.3[c]	10.7 ± 0.4[c]
	60	0.0	10.7 ± 0.3[a]	1.5 ± 0.2[d]	12.2 ± 0.5[b]
	120	0.0	9.9 ± 0.8[a]	2.5 ± 0.7[c]	12.4 ± 0.0[b]

Values are means ± SD. Values with different letters in the same column are significantly different at $p < 0.05$.
APBS: Amylopection-only barley starch; NBS: Normal barley starch; AMBS: Amylose-only barley starch.

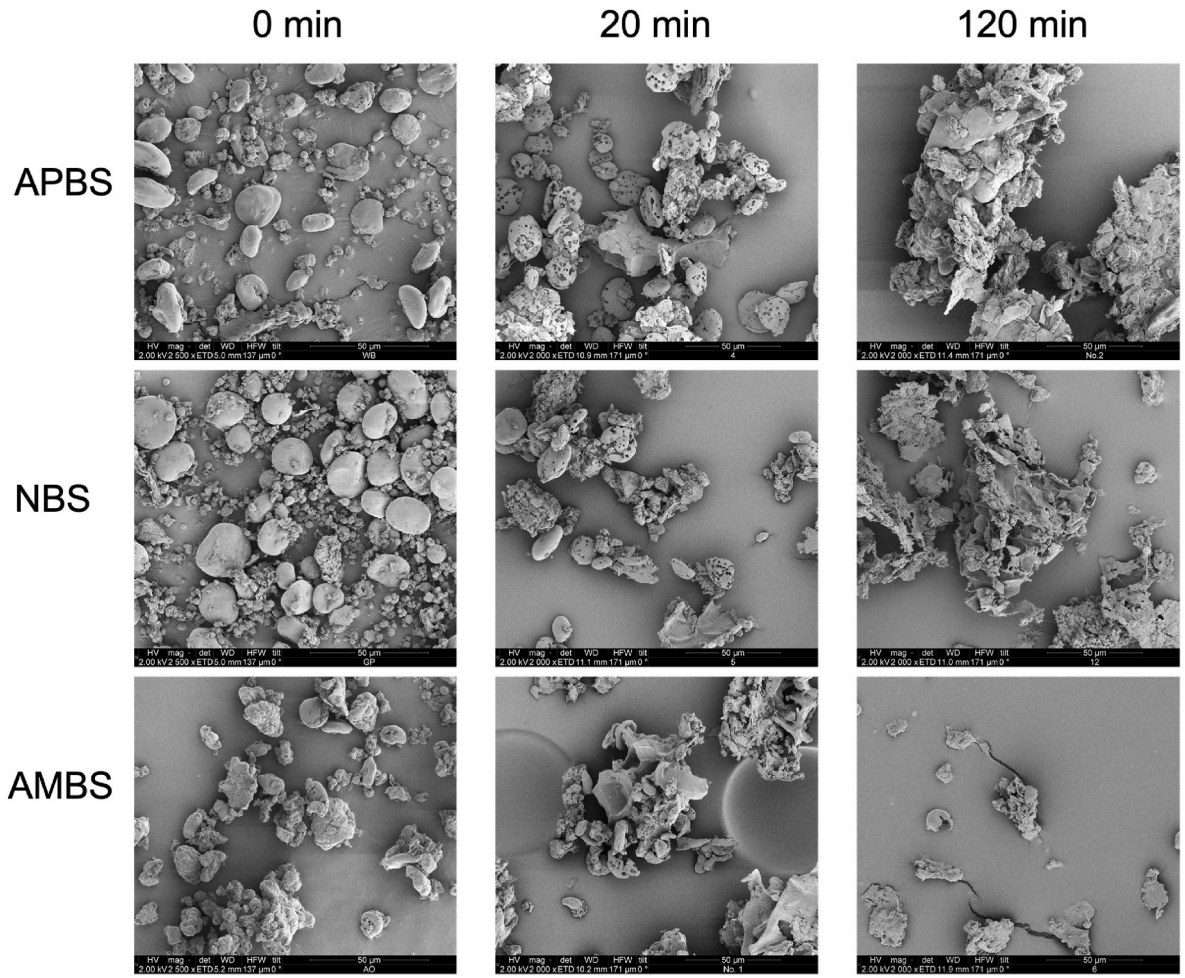

Fig. 7. The morphology of digested barley starches with different amylose content as analyzed by SEM. Abbreviations as in Fig. 1.

3.6. Schematic model of structural changes of barley starches during digestion

Based on the above data and their discussion, the structural changes of the three types of barley starches with different AC have been schemed (Fig. 8). During the first digestion stage of APBS, the amorphous and crystalline regions are both attacked by the enzymes, and AP side chains and backbone chains are hydrolyzed into smaller chains (DP ≤ 12), thereby loosening the crystalline and amorphous lamellae. Most crystals are, however, retained, although some double helices are hydrolyzed. However, new double helices are formed by cleaved AP backbone chains. At the second digestion stage, AP chains are further hydrolyzed, contributing to the formation of highly branched oligosaccharides, the disordered alignment of double helices, and the loss of the

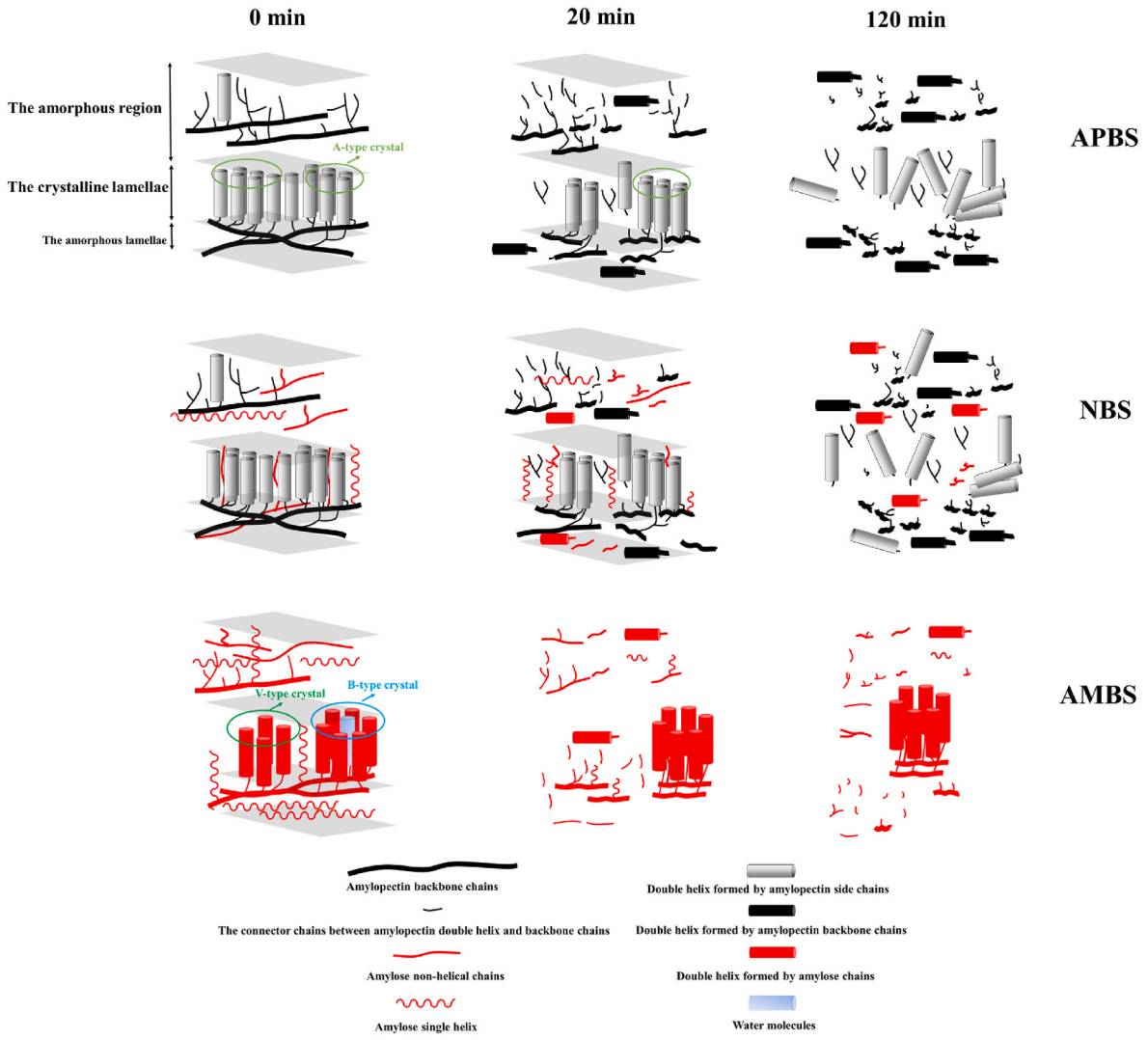

Fig. 8. Schematic temporal digestion models of barley starch with a full range difference in amylose content. APBS: Amylopection-only barley starch; NBS: Normal barley starch; AMBS: Amylose-only barley starch.

crystal and lamellar structures. The structural changes of NBS were similar to those observed for APBS. However, the higher amount of AM results in more AM single helices formed at the first digestion stage that are digested at the second digestion stage. AM double helices might also have been formed during the digestion process in the presence of newly formed AP double helices. This is evident in the AMBS system. The less ordered lamellar structure of AMBS, as compared to APBS and NBS, is rapidly lost at the initial digestion stage, and the single helix- and amorphous-state AM molecules are hydrolyzed into smaller segments while B-type crystals remain. These cleaved AM molecules have higher mobility, thereby forming new AM double helices. With increased digestion time, AM molecules are further hydrolyzed; however, AM double helices at a slower rate.

3.7. The mechanism of the low digestibility of AMBS

It is known that increasing AM content significantly elevates the resistant starch content in maize (Zhong, Tai, et al., 2022). It has been revealed that the high AM maize starch granules, Gelose 50 and Gelose 80, are resistant to enzymatic digestion due to their smooth granular surface and the maintenance of the granular integrity during digestion (Shrestha et al., 2012). However, the raw AMBS granules had a rough granular surface, and their granular structure was disrupted rapidly during digestion. Hence, the raw AMBS granules, possibly due to their rough surface, were initially highly susceptible to amylolytic digestion. In contrast, the reorganized aggregates consisting of short AM segments exhibited a high enzymatic resistance. Starch digestibility can be reduced as a function of its helical content (Y. Chen, Xie, et al., 2017), the degree of crystallinity (Zeng et al., 2014), and the degree of order of the lamellar structure (Chi et al., 2021). However, our data showed that AMBS had a lower helical content, and a more disordered crystalline and lamellar structure than APBS and NBS, indicating a low digestion resistance of its internal structure. A possible explanation for the low amylolytic susceptibility of reorganized AMBS granules is that the granular surface of the reorganized surface structure exhibited fewer binding sites for the digesting enzymes to act upon, resulting in (1) a reduced surface modification and, as a consequence, (2) a limited exposure of the internal granular structure to hydrolases. This is supported by SEM studies of APBS and NBS. Digestion is initiated by surface hydrolysis, and the generation of pores and channels allows for the diffusion of enzymes into the granular internal regionsand attacking the internal structure. However, in the final digestion period (120 min), when their internal structure ordering was lost, i.e., loss of lamellar structure, reorganization and aggregation of the hydrolyzed AP chains commenced (120 min digested APBS and NBS, Fig. 7), gaining a high enzymatic resistance (the digestion profiles of the two starches from 80

min to 120 min). Such enzymatic resistant aggregated structures were formed in the initial digestion stage of AMBS. Therefore, it is suggested that the enzymatic resistance of these granular AMBS structures is mainly related to the granular structure of starch and reorganized surface with limited hydrolase binding sites.

It has been reported that AM with different chain lengths exhibit different reorganization capabilities, and short AM chains are suggested to produce hydrolytically resistant structures more efficiently than long AM chains as they are forming more flexible and densely packed aggregates (Gong, Cheng, Gilbert, & Li, 2019). Hence, it is concievable that cleaved AM molecules in the first digestion stage showed a stronger reorganization capacity than the original AM molecules in the raw starch. Unfortunately, AMBS has never been compared with other common high-AM starch types, e.g., Gelose 80 and Hylon VII, by using the same structural analytical techniques, making direct comparison of differences in AM structure and digestibility problematic. It is expected that such a comparison will be performed in the future. On the other hand, the protein content in barley is high (8%–30%) (Jaeger, Zannini, Sahin, & Arendt, 2021), and it has been reported that proteins locate on (coating) granular surfaces and internal pores, and that discrete protein bodies deposite around starch granules in grains (Dhital, Brennan, & Gidley, 2019). Due to the strong ability of the AM-starch matrix to lower starch digestion by affecting the digestion rate constant (Li, Li, Fox, Gidley, & Dhital, 2021), it is also expected that residual protein in starch can form a complex with leached AM molecules in AMBS, thereby enhancing the digestion resistance of AMBS granules. Conceivably, this might be ture for AMBS from other crops as well, but this remains to be tested once these have been produced

The digestion process of three barley starches has been schemed in Fig. 8 on the basis of data in this study. Although APBS and NBS exhibited differences in their multi-scale structure, e.g., branching degree and the content of double helices (Table 2), the two types of starch had a similar digestion process. In the rapid digestion stage, the amorphous region was severely attacked in which the starch molecules were cleaved into smaller segments, and the crystalline region was less attacked, reflected as the remained ordered alignment of the double helices and the presence of a less ordered lamellar and crystalline structure. During the second digestion stage, the lamellar and crystalline structure was completely destroyed due to the further degradation of AP side chains (Fig. 3), especially for chains with DP 18–35 which are regarded as connector chains between the double helix and backbone chains (Zhong, Bertoft, Li, Blennow, & Liu, 2020). However, the remaining, and even increasing, content of double helices at this stage suggests that the non-double helix-related chains were primarily attacked and/or new double helical structures formed due to molecular reorganization. As for AMBS, the lamellar and crystalline structure disappeared during the first digestion stage, and a single helix structure was attacked, as the AM granular aggregation structure was apparently not stable. However, most crystals remained. At the next stage, the flexible AM molecules and the rest of the single helices were further attacked. However, the cleaved AM chains possibly reorganized thereby limiting exposure of the internal granular structure to hydrolases, retarding the rate of digestion.

4. Conclusions

The different amylolytic susceptibilities of barley starches with different AM content and the resulting consequences for the multi-scale structure of the starch were investigated in this study. The double helical structure was maintained throughout the digestion process, whereas single helices were digested faster. The AC was positively correlated with the amylolytically induced collapse of the lamellar structure and negatively correlated with the crystalline structure. Digestion of APBS and NBS resulted in the formation of porous granules within the first 20 min, followed by complete granular collapse and the aggregation of granular residues after 120 min. The granular integrity of AMBS was thoroughly disrupted at the initial 20 min digestion stage, and granular residues aggregated immediately thereafter. Such aggregated digestion residues were resistant to enzymatic digestion, and the generation of such structures at the initial stage of digestion seems to be critical for the low digestibility of AMBS. However, the underlying formation mechanism of these high-resistance aggregates is still unclear and requires further investigation of other types of AMBS granules.

Author statement

Wenxin Liang: Conceptualization, Investigation, Methodology, Software, Writing - Original Draft, Writing - Review & Editing.

Li Ding: Investigation, Methodology, Software, Writing - Original Draft, Writing - Review & Editing.

Ke Guo: Methodology, Software, Conceptualization.

Yang Liu: Conceptualization, Funding acquisition, Supervision.

Xiaoxia Wen: Conceptualization, Funding acquisition, Supervision.

Jacob Judas Kain Kirkensgaard: WAXS and SAXS analysis.

Bekzod Khakimov: 1H NMR analysis.

Kasper Enemark-Rasmussen: 13C NMR analysis.

Kim Henrik Hebelstrup: Material provider.

Klaus Herburger: Writing - Original Draft, Writing - Review & Editing.

Xingxun Liu: Writing - Original Draft, Writing - Review & Editing.

Staffan Persson: Funding acquisition, Writing - Review & Editing.

Andreas Blennow: Resources, Conceptualization, Funding acquisition, Supervision, Writing - Review & Editing.

Yuyue Zhong: Resources, Conceptualization, Funding acquisition, Supervision, Writing - Review & Editing.

Declaration of competing interest

The authors declare that there is no conflict of interests regarding the publication of this paper.

Data availability

Data will be made available on request.

Acknowledgments

This work was supported by HIAMBA - grain, flour, bread & bakery products preventing type 2 diabetes" Innovation Fund Denmark. Project 9067-00004A and Wenxin Liang also thank the China Scholarship Council (CSC) (201906300041) for support. S.P. acknowledges Villum Investigator (Project ID: 25915), DNRF Chair (DNRF155) and Novo Nordisk Laureate (NNF19OC0056076), Novo Nordisk Emerging Investigator (NNF20OC0060564) and Lundbeck foundation (Experiment grant, R346-2020-1546) grants.

Appendix A. Supplementary data

Supplementary data to this article can be found online at https://doi.org/10.1016/j.foodhyd.2023.108491.

References

Ao, Z., Simsek, S., Zhang, G., Venkatachalam, M., Reuhs, B. L., & Hamaker, B. R. (2007). Starch with a slow digestion property produced by altering its chain length, branch density, and crystalline structure. *Journal of Agricultural and Food Chemistry, 55*(11), 4540–4547.

Baik, B. K., & Ullrich, S. E. (2008). Barley for food: Characteristics, improvement, and renewed interest. *Journal of Cereal Science, 48*(2), 233–242.

Bertoft, E. (2017). Understanding starch structure. *Recent Progress, 7*(3), 56.

Butterworth, P. J., Warren, F. J., & Ellis, P. R. (2011). Human α-amylase and starch digestion: An interesting marriage. *Starch-Stärke, 63*(7), 395–405.

Carciofi, M., Blennow, A., Jensen, S. L., Shaik, S. S., Henriksen, A., Buléon, A., et al. (2012), 1. In *Concerted suppression of all starch branching enzyme genes in barley produces amylose-only starch granules* (Vol. 12, p. 223), 223.
Chen, P., Xie, F., Zhao, L., Qiao, Q., & Liu, X. (2017). Effect of acid hydrolysis on the multi-scale structure change of starch with different amylose content. *Food Hydrocolloids, 69*, 359–368.
Chen, Y., Yang, Q., Xu, X., Qi, L., Dong, Z., Luo, Z., et al. (2017). Structural changes of waxy and normal maize starches modified by heat moisture treatment and their relationship with starch digestibility. *Carbohydrate Polymers, 177*, 232–240.
Chi, C., Li, X., Huang, S., Chen, L., Zhang, Y., Li, L., et al. (2021). Basic principles in starch multi-scale structuration to mitigate digestibility: A review. *Trends in Food Science & Technology, 109*, 154–168.
Dhital, S., Brennan, C., & Gidley, M. J. (2019). Location and interactions of starches in planta: Effects on food and nutritional functionality. *Trends in Food Science & Technology, 93*, 158–166.
Gidley, M. J. (1985). Quantification of the structural features of starch polysaccharides by n.m.r. spectroscopy. *Carbohydrate Research, 139*, 85–93.
Gilles, C., Astier, J. P., Marchis-Mouren, G., Cambillau, C., & Payan, F. (1996). Crystal structure of pig pancreatic α-amylase isoenzyme II, in complex with the carbohydrate inhibitor acarbose. *European Journal of Biochemistry, 238*(2), 561–569.
Gong, B., Cheng, L., Gilbert, R. G., & Li, C. (2019). Distribution of short to medium amylose chains are major controllers of in vitro digestion of retrograded rice starch. *Food Hydrocolloids, 96*, 634–643.
Guo, J., Tan, L., & Kong, L. (2021). Impact of dietary intake of resistant starch on obesity and associated metabolic profiles in human: A systematic review of the literature. *Critical Reviews in Food Science and Nutrition, 61*(6), 889–905.
Jaeger, A., Zannini, E., Sahin, A. W., & Arendt, E. K. (2021). Barley protein properties, extraction and applications, with a focus on brewers' spent grain protein. *Foods, 10*(6), 1389.
Jiang, H., Campbell, M., Blanco, M., & Jane, J.-L. (2010). Characterization of maize amylose-extender (ae) mutant starches: Part II. Structures and properties of starch residues remaining after enzymatic hydrolysis at boiling-water temperature. *Carbohydrate Polymers, 80*(1), 1–12.
Khakimov, B., Mobaraki, N., Trimigno, A., Aru, V., & Engelsen, S. B. (2020). Signature Mapping (SigMa): An efficient approach for processing complex human urine ^{1}H NMR metabolomics data. *Analytica Chimica Acta, 1108*, 142–151.
Klucinec, J. D., & Thompson, D. B. (1999). Amylose and amylopectin interact in retrogradation of dispersed high-amylose starches. *Cereal Chemistry, 76*(2), 282–291.
Kuang, Q., Xu, J., Liang, Y., Xie, F., Tian, F., Zhou, S., et al. (2017). Lamellar structure change of waxy corn starch during gelatinization by time-resolved synchrotron SAXS. *Food Hydrocolloids, 62*, 43–48.
Li, P., Dhital, S., Zhang, B., He, X., Fu, X., & Huang, Q. (2018). Surface structural features control in vitro digestion kinetics of bean starches. *Food Hydrocolloids, 85*, 343–351.
Li, H., Gidley, M. J., & Dhital, S. (2019). High-amylose starches to bridge the "fiber gap": Development, structure, and nutritional functionality. *Comprehensive Reviews in Food Science and Food Safety, 18*(2), 362–379.
Li, C., Hu, Y., Gu, F., & Gong, B. (2021). Causal relations among starch fine molecular structure, lamellar/crystalline structure and in vitro digestion kinetics of native rice starch. *Food & Function, 12*(2), 682–695.
Li, L., Jiang, H., Campbell, M., Blanco, M., & Jane, J.-l. (2008). Characterization of maize amylose-extender (ae) mutant starches. Part I: Relationship between resistant starch contents and molecular structures. *Carbohydrate Polymers, 74*(3), 396–404.
Ma, Z., Yin, X., Hu, X., Li, X., Liu, L., & Boye, J. I. (2018). Structural characterization of resistant starch isolated from Laird lentils (Lens culinaris) seeds subjected to different processing treatments. *Food Chemistry, 263*, 163–170.
Noor, N., Gani, A., Jhan, F., Jenno, J. L. H., & Arif Dar, M. (2021). Resistant starch type 2 from lotus stem: Ultrasonic effect on physical and nutraceutical properties. *Ultrasonics Sonochemistry, 76*, Article 105655.
Shrestha, A. K., Blazek, J., Flanagan, B. M., Dhital, S., Larroque, O., Morell, M. K., et al. (2012). Molecular, mesoscopic and microscopic structure evolution during amylase digestion of maize starch granules. *Carbohydrate Polymers, 90*(1), 23–33.
Shaik, S. S., Obata, T., Hebelstrup, K. H., Fernie, A. R., Mateiu, R. V., & Blennow, A. (2016). Alterations in starch branching enzyme and glucan water dikinase: Effects on grain physiology and metabolism. *PLoS ONE, 11*(2). https://doi.org/10.1371/journal.pone.0149613. e0149613, 2016.
Song, Z., Zhong, Y., Tian, W., Zhang, C., Hansen, A. R., Blennow, A., et al. (2020). Structural and functional characterizations of α-amylase-treated porous popcorn starch. *Food Hydrocolloids, 108*, Article 105606.
Tan, I., Flanagan, B. M., Halley, P. J., Whittaker, A. K., & Gidley, M. J. (2007). A method for estimating the nature and relative proportions of amorphous, single, and double-helical components in starch granules by 13C CP/MAS NMR. *Biomacromolecules, 8*(3), 885–891.
Witt, T., Gidley, M. J., & Gilbert, R. G. (2010). Starch digestion mechanistic information from the time evolution of molecular size distributions. *Journal of Agricultural and Food Chemistry, 58*(14), 8444–8452.
Wu, A. C., Morell, M. K., & Gilbert, R. G. (2013). A parameterized model of amylopectin synthesis provides key insights into the synthesis of granular starch. *PLoS One, 8*(6), Article e65768.
Yao, M., Tian, Y., Yang, W., Huang, M., Zhou, S., & Liu, X. (2019). The multi-scale structure, thermal and digestion properties of mung bean starch. *International Journal of Biological Macromolecules, 131*, 871–878.
Zeng, F., Ma, F., Gao, Q., Yu, S., Kong, F., & Zhu, S. (2014). Debranching and temperature-cycled crystallization of waxy rice starch and their digestibility. *Carbohydrate Polymers, 113*, 91–96.
Zeng, Y., Pu, X., Yang, J., Du, J., Yang, X., Li, X., et al. (2018). Preventive and therapeutic role of functional ingredients of barley grass for chronic diseases in human beings. *Oxidative Medicine and Cellular Longevity, 2018*.
Zhang, G., Sofyan, M., & Hamaker, B. R. (2008). Slowly digestible state of starch: Mechanism of slow digestion property of gelatinized maize starch. *Journal of Agricultural and Food Chemistry, 56*(12), 4695–4702.
Zhong, Y., Bertoft, E., Li, Z., Blennow, A., & Liu, X. (2020). Amylopectin starch granule lamellar structure as deduced from unit chain length data. *Food Hydrocolloids, 108*, Article 106053.
Zhong, Y., Herburger, K., Kain Kirkensgaard, J. J., Khakimov, B., Hansen, A. R., & Blennow, A. (2021). Sequential maltogenic α-amylase and branching enzyme treatment to modify granular corn starch. *Food Hydrocolloids*, Article 106904.
Zhong, Y., Herburger, K., Xu, J., Kirkensgaard, J. J. K., Khakimov, B., Hansen, A. R., et al. (2022). Ethanol pretreatment increases the efficiency of maltogenic α-amylase and branching enzyme to modify the structure of granular native maize starch. *Food Hydrocolloids, 123*, Article 107118.
Zhong, Y., Keeratiburana, T., Kain Kirkensgaard, J. J., Khakimov, B., Blennow, A., & Hansen, A. R. (2021). Generation of short-chained granular corn starch by maltogenic α-amylase and transglucosidase treatment. *Carbohydrate Polymers, 251*, Article 117056.
Zhong, Y., Li, Z., Qu, J., Bertoft, E., Li, M., Zhu, F., et al. (2021). Relationship between molecular structure and lamellar and crystalline structure of rice starch. *Carbohydrate Polymers, 258*, Article 117616.
Zhong, Y., Liu, L., Qu, J., Blennow, A., Hansen, A. R., Wu, Y., et al. (2020). Amylose content and specific fine structures affect lamellar structure and digestibility of maize starches. *Food Hydrocolloids*, Article 105994.
Zhong, Y., Liu, L., Qu, J., Li, S., Blennow, A., Seytahmetovna, S. A., et al. (2020). The relationship between the expression pattern of starch biosynthesis enzymes and molecular structure of high amylose maize starch. *Carbohydrate Polymers*, Article 116681.
Zhong, Y., Qu, J. Z., Liu, X., Ding, L., Liu, Y., Bertoft, E., et al. (2022). Different genetic strategies to generate high amylose starch mutants by engineering the starch biosynthetic pathways. *Carbohydrate Polymers, 287*, Article 119327.
Zhong, Y., Tai, L., Blennow, A., Ding, L., Herburger, K., Qu, J., et al. (2022). High-amylose starch: Structure, functionality and applications. *Critical Reviews in Food Science and Nutrition*, 1–23.
Zhong, Y., Tian, Y., Liu, X., Ding, L., Kirkensgaard, J. J. K., Hebelstrup, K., et al. (2021). Influence of microwave treatment on the structure and functionality of pure amylose and amylopectin systems. *Food Hydrocolloids, 119*, Article 106856.
Zhong, Y., Xu, J., Liu, X., Ding, L., Svensson, B., Herburger, K., et al. (2022). Recent advances in enzyme biotechnology on modifying gelatinized and granular starch. *Trends in Food Science & Technology, 123*, 343–354.